Werk

Jahr: 1982
Kollektion: fid.geo
Signatur: 8 Z NAT 2148:51
Digitalisiert: Niedersächsische Staats- und Universitätsbibliothek Göttingen
Werk Id: PPN1015067948_0051
PURL: http://resolver.sub.uni-goettingen.de/purl?PPN1015067948_0051

LOG Id: LOG_0026
LOG Titel: Source parameters of mine tremors in the eastern part of the Ruhr-District (West-Germany)
LOG Typ: article

Übergeordnetes Werk

Werk Id: PPN1015067948
PURL: http://resolver.sub.uni-goettingen.de/purl?PPN1015067948
OPAC: http://opac.sub.uni-goettingen.de/DB=1/PPN?PPN=1015067948

Contact

Niedersächsische Staats- und Universitätsbibliothek Göttingen
Georg-August-Universität Göttingen
Platz der Göttinger Sieben 1
37073 Göttingen
Germany
Email: gdz@sub.uni-goettingen.de

Source Parameters of Mine Tremors in the Eastern Part
of the Ruhr-District (West-Germany)

K.-G. Hinzen

Institut für Geophysik der Ruhr-Universität Bochum,
Universitätsstraße 150, D-4630 Bochum 1, Federal Republic of Germany

Abstract. About 190 mine tremors were recorded during a 120 day period in the eastern part of the Ruhr-district (West Germany). Source parameters of 37 tremors $(1.3 \leqq M_L \leqq 2.3)$ are calculated. Hypocentral distance was about 2 km. A combined plot of first P-wave motions in an equal area projection of a focal sphere possibly suggests a dip slip mechanism. Displacement P-wave spectra of 13 events show a clear low frequency level and a high frequency asymptotic behaviour as f^{-3}, where f is the frequency. Seismic moment varies from 2.3×10^{18} dyn cm to 2.3×10^{19} dyn cm. Corner frequencies are in the range of 12–16 Hz. Interpretation of spectra with Brune's (1970) model extended by Hanks and Wyss (1972) leads to source dimensions between 87 m and 120 m. Stress drops vary from 0.9 bars to 8.4 bars. Average dislocations range from 0.6 mm to 19 mm. Stress drop, dislocation, and seismic moment have a clear dependence on radiated seismic energy. Seismic energy of the mine tremors is between 1.4 $\times 10^{13}$ ergs and 2.2×10^{15} ergs. The energy magnitude relation $\log E = 11.8 + 1.5 M$ given by Gutenberg and Richter is in good agreement with the data.

Source dimensions are in the same range as those found for mine tremors in Utah, South Africa, and Poland.

Key words: Mining induced seismicity – Mine tremors – Source dimensions – Stress drop

Introduction

Since Reid (1910) made his geodetic studies of the 1906 San Francisco earthquake, a shear fault mechanism has been the most comonly used earthquake model. A great variety of kinematic and dynamic models have been developed in the past. Many models permit the determination of source parameters from farfield measurements of seismic waves, especially from displacement spectra (Kasahara 1957; Archambeau 1964; Berckhemer and Jacob 1968; Brune 1970; Hanks and Wyss 1972; Madariaga 1976; Boatwright 1980).

In this connection, mine tremors are an interesting subject of study. It would be important to the mining industry, if the same models used for natural earthquakes could be applied to mine tremors. Conversely, mine tremors could be used as "model earthquakes" in order to study different techniques of source parameter determination.

Some attempts have been made to analyze the focal mechanism of mine tremors. Tremors induced by coal mining in Utah, USA, have been studied by Smith et al. (1974). Spottiswoode and McGarr (1975) and McGarr et al. (1981) examined tremors in a deep level gold mine of South Africa. Source studies of Polish coal mine tremors have been made by Gibbowicz and Chichowicz (1977).

In this study source parameters of coal mine tremors from the Ruhr-District (West Germany) are determined and compared with other induced seismic events.

In none of the studies mentioned above was the shear dislocation model contrary to the observations. In addition, inspection in a South African gold mine by McGarr et al. (1979) showed some shear zones caused by mine-tremors. Combined fault-plane-solutions of mine tremors in eastern Utah (Smith et al. 1974) and in Stoke-on-Trent, UK (Westbrook et al. 1980) show that some of the mine tremors were of strike-slip mechanism.

Instrumentation

Five vertical seismometers (Baule-Hottinger B 5 Z) with natural frequencies of 2.5 Hz and at 62% of critical damping were used to record ground velocity. The seismometer locations are shown in Fig. 1.

The signals were recorded at a central station. Event recording was made with a six channel pulse-code-modulating unit. Signals were recorded continuously on a three channel ink recorder. The dynamic range of the event recording system was 60 dB.

Data

From Dec. 1978 to Sept. 1980 a local seismic network of 5 stations operated in the eastern part of the Ruhr-district (West Germany). In the period from January 1st, 1979 to April 30th, 1979 a series of about 190 mine tremors was recorded and about 60 of these were recorded on magnetic tape (Baule and Hinzen 1981).

Most of the events were detected at stations 2, 3, 4 and 5 (see Fig. 1). Station 5 consistently showed the best signal to noise ratio while the seismograms at
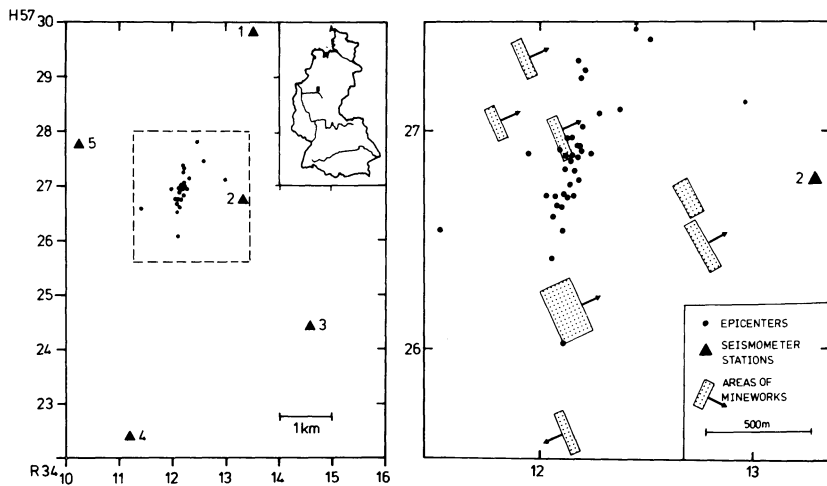
Fig. 1. Location of seismometers No. 1 to 5 (▲) and epicenters of mine tremors (●) are shown on the left. Coordinates are from the third stripe of the Gauss-Krüger-Net. The *insert* is a map of West Germany with the location of the focal area (■). The area within the *dashed lines* is shown in detail on the rigth. Epicenters are given in relation to mining activity
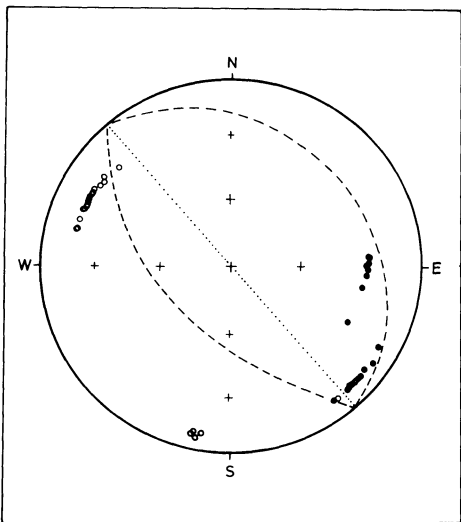

Fig. 2. Observed *P*-wave first motions of 21 events in an equal area projection of the upper focal sphere. *Open circles* are dilatations, *closed circles* are compressions. Two possible fault plane solutions are indicated: a dip slip mechanism with a vertical NW–SE striking fault plane (*dotted line*) and a thrust fault with NW–SE striking fault planes (*dashed lines*)

station 2 were clipped. Thirty-seven seismograms from station 5 were used to determine source parameters.

Epicenter locations were made with a ray-tracing routine (Pelzing 1978) and are shown in Fig. 1. The epicentral distance to the tremors was about 2 km. Determination of the focal depth was not possible in most cases because a clear onset could only be read in the seismograms of three stations. Past experience has shown that most of the tremors in the Ruhr-district are located above the mine workings, which are about 900 m below the surface in our case, so a constant depth of 750 m was assumed as focal depth for all events. This assumption is not critical as it affects only slightly the hypocentral distance; a mistake of 250 m in depth causes only a 5 % change.

Fault Plane Solution

In our case the number of stations was too small to construct fault-plane solutions but a combined analysis

of a large swarm of tremors from the same mine allows some conclusions.

Figure 2 shows the observed *P*-wave first motions for 21 events. The scatter of data in the equal area projection is caused by the variation of epicenters and perhaps by variation in focal mechanisms as well. At the north-western and southern station only dilatational *P*-wave first motions were observed (open circles). The station in the east shows only compression (closed dircles). At the station in the south-east compressional and dilatational *P*-wave first motions are measured. This may indicate that the station is located close to a nodal plane. In this case, a simple dip-slip mechanism with a vertical NW-SE striking fault plane (dotted line) and a thrust fault with NW-SE striking fault planes (dashed lines) are possible solutions. Due to the uncertainties of these fault plane solutions, the stress axes are not derived.

Even if a poor S/N ratio caused the ambiguous polarity at the station in the south-east, an implosive source cannot explain the measurements. A shear fault is a more probable model for the mine tremors analyzed in this study.

Magnitude Determination

Local magnitudes M_L of the events were calculated from seismograms recorded at the seismic station of the Ruhr-University in Bochum (BUG). The epicentral distance of this station is about 40 km. The displacement response of the three component short period transducers (Baule-Hottinger B4) is very similar to that of a Wood-Anderson standard seismograph. The product of the inverse amplitude response of the short period instruments at $BUG (AR_{BUG})^{-1}$ and the amplitude response of Wood-Anderson seismograph, AR_{WA} was calculated. After correcting for the actual gain M_L is easily determined from the largest trace amplitude. The correction factor for amplitudes is given by $AR_{WA} \cdot (AR_{BUG})^{-1}$. The range of measured magnitudes is: $1.28 \leq M_L \leq 2.3$.

Seismic Energy

Taking geometrical spreading and seismic impedance into account, the seismic energy E is given by:

$$E = 4\pi R^2 \rho c \int_{t1}^{t2} v_c^2(t)\, dt \qquad (1)$$

where ρ is the density, R is the hypocentral distance and $v_c(t)$ the ground velocity of the P- or S-phase ($c = \alpha, \beta$). Perret (1972) has shown that this calculation is valid for spherically symmetrical radiation and $R \gg c/f$, where f is the frequency. In this study c/f is always smaller than 500 m and the hypocentral distance is in the range of 2 km.

Energy was determined using the P-arrival, because only vertical components were available. Fortunately P-waves are less sensitive to attenuation than S-waves (Wyss 1970). Regarding the energy of the S-wave, amplitudes of the S-waves were assumed to be three times larger than those of P-waves (Haskell 1964; Archambeau 1964).

Energy Accumulation and Energy Release

The energy accumulation for the 120 day period is plotted in Fig. 3. All events recorded on the ink recorder were used.

Three stages of different energy accumulation rate $d\Sigma E/dt$ are obvious:

1. period: $0 \leq t \leq 34$ (in days)

$$\frac{d\Sigma E}{dt} = 0.27 \times 10^{15}\ \text{erg/day}$$

2. period: $34 < t \leq 59$

$$\frac{d\Sigma E}{dt} = 0.55 \times 10^{15}\ \text{erg/day}$$

3. period: $59 < t \leq 101$

$$\frac{d\Sigma E}{dt} = 0.08 \times 10^{15}\ \text{erg/day}$$

The total energy release, E_{tot}, for the 120 day period is

$$\Sigma E_{tot} = 2.5 \times 10^{16}\ \text{erg}$$

with a maximum rate during the second period.

In Fig. 3 there is also shown the cumulative number of events which correlates well with energy release. The number of events per day $d\Sigma N/dt$ is:

1. stage: $9 \leq t \leq 34$ (in days)

$$d\Sigma N/dt = 0.8\ \text{day}^{-1}$$

2. stage: $34 < t \leq 69$

$$d\Sigma N/dt = 4.4\ \text{day}^{-1}$$

3. stage: $69 < t \leq 99$

$$d\Sigma N/dt = 1.14\ \text{day}^{-1}$$

Energy-Magnitude Relation

The relation between seismic energy, E, and local magnitude, M_L, is shown in Fig. 4. The relationship given by Gutenberg and Richter (1956)
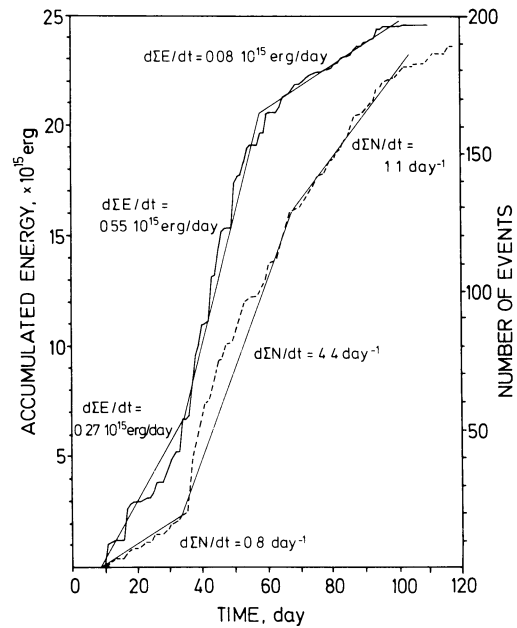
$$\log E = 11.8 + 1.5 M \qquad (2)$$

Fig. 3. Cumulative diagram of released seismic energy (*continuous line*) and number of events (*dashed line*). Thin straight lines give mean values of $d\Sigma E/dt$ and $d\Sigma N/dt$ for three periods
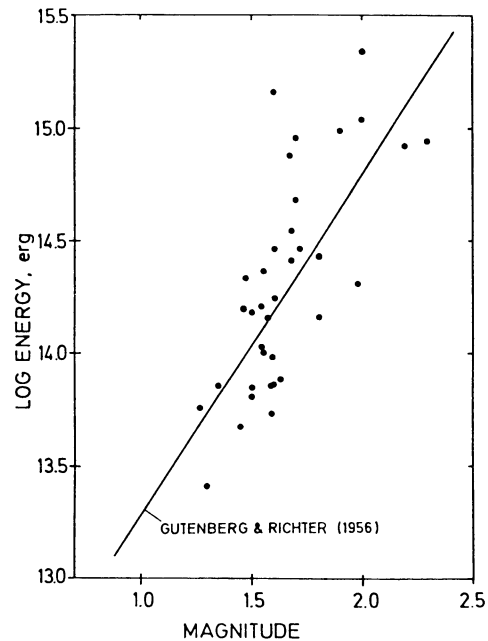
Fig. 4. Energy-magnitude relationship. Local magnitudes were calculated from seismograms recorded at Station BUG. *Solid curve* is the relation given by Gutenberg and Richter (1956)

which was developed for the surface wave magnitude scale, provides a good fit to the data. Although the scatter and the small magnitude range limits our data sample, other relations given by Thatcher and Hanks (1973)

$$\log E = 8.1 + 2.0 M \qquad (3)$$
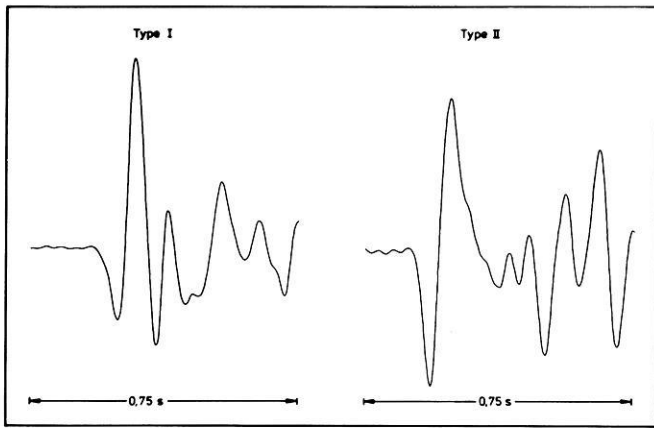
and Richter (1958)

Fig. 5. Comparison of two different types of *P*-pulses

$$\log E = 9.9 + 1.9 M_{\mathrm{L}} - 0.024 M_{\mathrm{L}}^2 \qquad (4)$$

do not agree with the data of this study. The energies calculated using Eqs. (3) and (4) are much smaller than those determined from the seismograms using the apparent stress. This agrees well with results from Aki (1980), who found that energies calculated from Eq. (4) were underestimated by about a factor of 10 for earthquakes with $M_{\mathrm{L}} \geqq 4.0$. Similar results were obtained by Spottiswoode and McGarr (1975) for tremors in a deep-level gold mine in South Africa.

Shape of *P*-Pulses

The *P*-pulses of the 37 events show two different types, which will be referred to as type I and II. 13 events are of type I and 22 of type II, two events cannot be classified.

Type I is dominated by a strong upward movement, which follows immediately after a small negative onset. It must be mentioned, that the small negative onset can not be explained by simple dislocation models like that of Brune (1970, 1971) which is used in this study. The amplitudes of the downward and upward movement are nearly the same for type II pulses. One example of each pulse is shown in Fig. 5. Because type II events cannot be explained by a shear dislocation, source parameters are only calculated for type I events.

Spectra of Ground Displacement

To determine displacement spectra the pulse-code modulated signals were demodulated and digitized. The sampling interval was $\Delta t = 5$ ms (Nyquist frequency $f_{\mathrm{NY}} = 100$ Hz). A possible DC-offset was removed. The velocity seismograms were corrected for instrument response and integrated to produce ground displacement. To separate the *P*-pulse, a Gaussian window

$$W(n) = \exp\left(-\left(\frac{2n}{N}\right)^2 \frac{\varepsilon^2}{2}\right) \qquad (5)$$

with $n = -N/2, \ldots, -1, 0, 1, \ldots, N/2$ was used.

ε is an adjustable parameter, the reciprocal standard deviation. A value of 3 was chosen for ε. The window length was adjusted to the length of the *P*-pulse; gener-
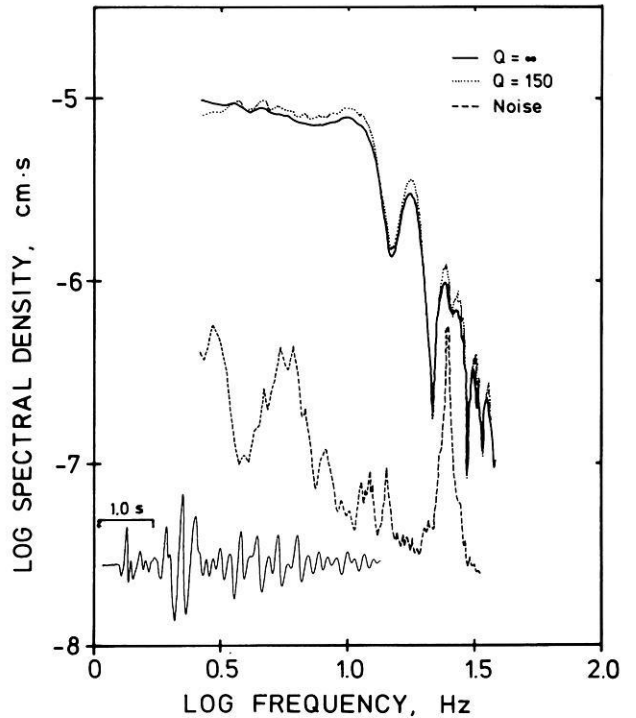

Fig. 6. Displacement spectrum of a *P*-pulse for $Q = \infty$ (*continuous line*) and $Q = 150$ (*dotted line*). The *insert* in the lower left shows the displacement seismogram with the bar indicating the analysed time interval. The *dashed line* is a noise spectrum of station No. 5

ally, it was about 150 samples with the window maximum in the middle of the *P*-pulse. For technical reasons, zeros had to be added up to 1,024 samples. Spectra were plotted on a logarithmic scale. Correction of the spectra for attenuation did not seem necessary due to the short hypocentral distance. The quality factor, Q, for *P*-waves in Carboniferous rocks ranges from 100–300 (Gibbowicz and Chichowicz 1977).

Figure 6 shows the measured spectra of a *P*-pulse (continuous line), the same spectra corrected for $Q = 150$ (dotted line) and a typical noise spectrum of station 5 (dashed line). The effect of the correction for attenuation is not significant. The sharp peak in the noise spectrum at a frequency of 25 Hz is caused by a ventilator in an air-shaft in the vicinity of station No. 5.

Figure 7 gives four examples of the displacement spectra. Low- and high-frequency asymptotes and corner frequencies are indicated and about one second of the transformed *P*-pulse is shown.

All spectra have a clear flat low-frequency part and a decreasing trend above the corner frequency f_0. To determine the zero frequency intercept, Ω_0, the corner frequency, f_0, and the rate of high-frequency decay, γ, some master curves were calculated. The curves are based on the empirical assumption of the general form of displacement spectra as presented for example by Brune (1970). The master curves have the form

$$\hat{U}_m = \frac{1}{1 + (f/f_0)^\gamma} \qquad \text{(Marion and Long, 1980).} \qquad (6)$$
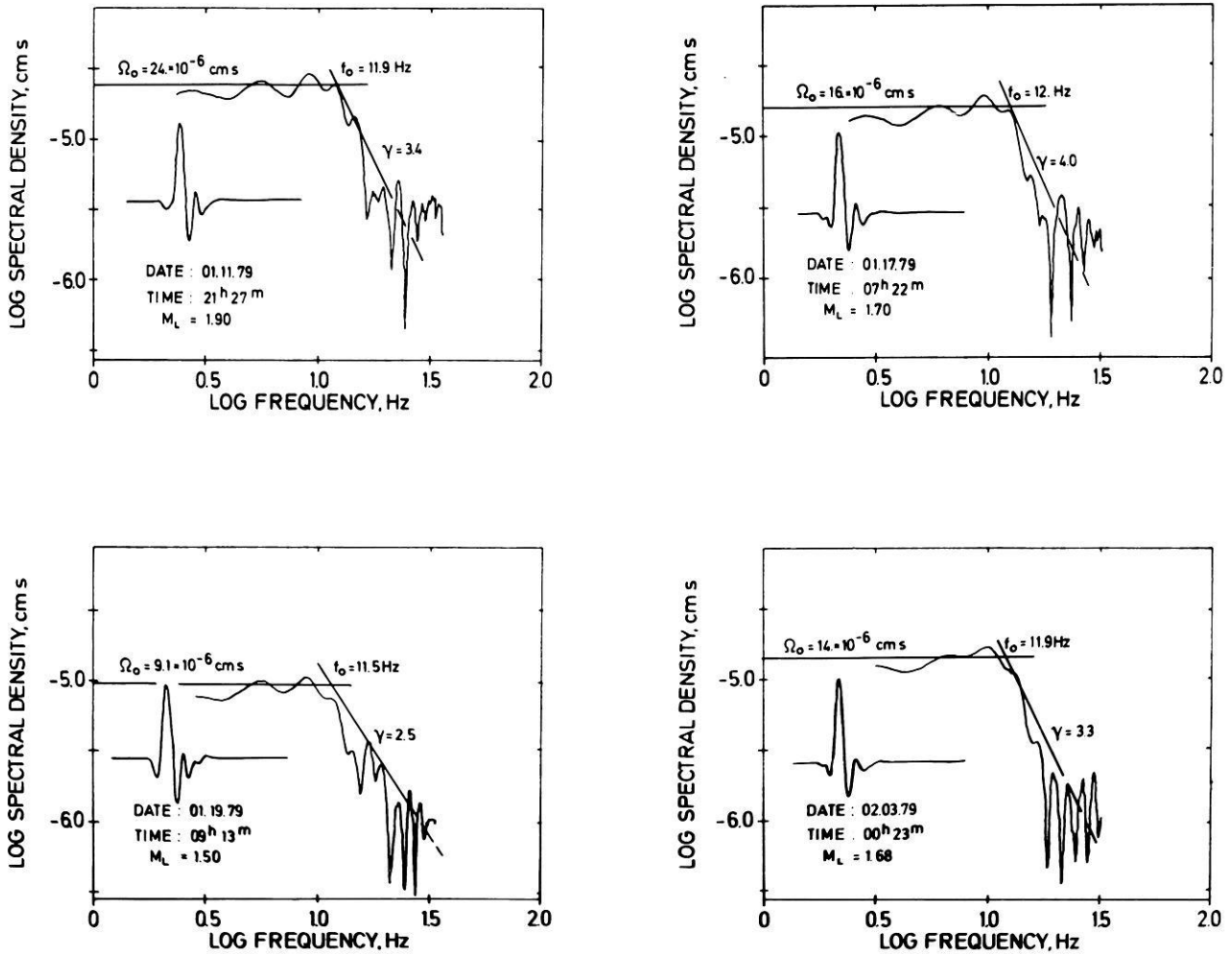
Fig. 7. Four examples of measured *P*-wave displacement spectra of seismograms from station 5 in log-log plots. High- and low-frequency asymptotes, Ω_0-values, rates of high-frequency decay, γ, and corner frequencies, f_0, are indicated. The *insert* gives the shape of the transformed *P*-pulse of 1s length

Vertical adjustment of the master curves to the measured spectra gives the low-frequency asymptote. Horizontal adjustment gives the corner frequency. γ is the curve parameter. The mean value of γ for all events is $\bar{\gamma} = 3.4 \pm 0.5$.

Source Parameters

For a double couple model the moment of one couple M_0 is related to the zero frequency intercept by:

$$M_0 = 4\pi\rho\alpha^3 R(A^{\text{FP}})^{-1}\Omega_0 \quad \text{(Keilis-Borok, 1960)} \tag{7}$$

where A^{FP} is the far field radiation pattern of *P*-waves, ρ is the density, α is the *P*-wave velocity, and R is the hypocentral distance. Because of the unknown focal mechanism a mean value $A^{\text{FP}} = 0.39$ was chosen for *P*-waves (Spottiswoode and McGarr, 1975). Density was assumed to be $\rho = 2.6\,\text{g/cm}^3$. The average *P*-wave velocity is known from blasting experiments to be $\alpha = 3,720\,\text{m/s}$.

Besides seismic moment Table 1 presents seismic energy, source dimension r_0, stress drop $\Delta\sigma_0$, and the average dislocation $\bar{d}_0$ for type I events.

The radius for a circular fault, r_0, in Brune's model (Brune 1970, 1971) is related to the corner frequency f_0 by

$$r_0 = \frac{2.34\alpha}{2\pi f_0^{(P)}} \quad \text{(Hanks and Wyss, 1972).} \tag{9}$$

The average dislocation is given by Aki (1966) as:

$$\bar{d}_0 = \frac{M_0}{\pi r_0^2\mu} \tag{10}$$

where the shear modulus μ was taken to be $\mu = 3 \times 10^{11}\,\text{dyn/cm}^2$. The stress drop was calculated using

$$\Delta\sigma_0 = \tfrac{7}{16}M_0/r_0^3 \tag{11}$$

following Brune (1970).

In Fig. 8 (from bottom to top) seismic moment, stress drop, average dislocation, and source dimension are plotted as a function of seismic energy for the 13 type I events.

Seismic moment of the mine tremors is between $2.3 \times 10^{18}\,\text{dyn cm}$ and $2.3 \times 10^{19}\,\text{dyn cm}$. The best linear relation between M_0 and E is:

$$M_0 = 0.6\log E + 10.1.$$

Table 1. Source parameters and local magnitudes of mine tremors in the eastern Ruhr district

Date	Time	E (10^{14} erg)	M_0 (10^{19} dyn cm)	r_0 (m)	$\Delta\sigma_0$ (bars)	d_0 (cm)	M_L	Type
11. 1. 79	$21^h 27^m$	9.76	2.30	116	6.4	0.18	1.9	I
17. 1. 79	07 22	4.80	1.50	115	4.3	0.12	1.7	I
19. 1. 79	09 13	1.55	0.89	120	2.2	0.07	1.5	I
23. 1. 79	08 40	1.76	0.92	104	3.6	0.09	1.6	I
26. 1. 79	19 30	7.65	1.70	114	5.0	0.14	1.7	I
29. 1. 79	21 16	2.63	1.00	108	3.5	0.09	1.7	I
3. 2. 79	00 23	3.58	1.40	116	3.9	0.11	1.7	I
3. 2. 79	13 18	8.80	–	–	–	–	2.3	II
5. 2. 79	17 08	0.57	0.51	101	2.2	0.05	1.3	I
6. 2. 79	16 53	11.00	–	–	–	–	2.0	I
6. 2. 79	22 29	2.36	0.78	103	3.1	0.08	1.6	II
7. 2. 79	07 42	0.14	–	–	–	–	–	?
9. 2. 79	00 40	0.45	0.23	98	0.9	0.02	–	I
14. 2. 79	03 40	0.59	9.39	87	2.6	0.06	–	I
14. 2. 79	09 30	14.60	–	–	–	–	1.9	?
19. 2. 79	11 11	21.90	–	–	–	–	2.0	II
20. 2. 79	12 04	2.23	0.83	95	4.2	0.10	1.5	I
22. 2. 79	10 55	8.41	1.50	92	8.4	0.19	2.2	I
27. 2. 79	22 26	9.25	–	–	–	–	1.7	II
27. 2. 79	22 36	1.08	–	–	–	–	1.5	II
1. 3. 79	22 34	2.06	–	–	–	–	2.0	II
5. 3. 79	11 19	0.65	–	–	–	–	1.5	II
6. 3. 79	23 21	2.73	–	–	–	–	1.8	II
7. 3. 79	17 17	0.78	–	–	–	–	1.6	II
9. 3. 79	01 08	0.73	–	–	–	–	1.6	II
10. 3. 79	02 11	1.45	–	–	–	–	1.8	II
12. 3. 79	11 58	2.96	–	–	–	–	1.7	II
13. 3. 79	01 27	0.79	–	–	–	–	1.6	II
14. 3. 79	18 05	0.54	–	–	–	–	1.6	II
15. 3. 79	18 58	1.60	–	–	–	–	1.5	II
16. 3. 79	15 14	0.72	–	–	–	–	1.4	II
17. 3. 79	14 17	0.48	–	–	–	–	1.4	II
19. 3. 79	14 48	0.26	–	–	–	–	1.3	II
22. 3. 79	05 49	1.62	–	–	–	–	1.5	II
29. 3. 79	21 23	1.02	–	–	–	–	1.6	II
31. 3. 79	01 01	1.49	–	–	–	–	1.6	II
2. 4. 79	17 51	0.71	–	–	–	–	1.5	II

Stress drop varies from 0.9 bar to 8.4 bar. A functional relation between E_s and stress drop is obvious. The best fit to the data is:

$$\log \Delta\sigma_0 = 0.5 \log E - 6.4.$$

The average dislocations – ranging from 0.2 to 19 mm – increase with increasing seismic energy:

$$\bar{d}_0 = 0.5 \log E - 8.6.$$

The source dimension varies from 87 to 120 m. A systematic relation between source dimension and radiated seismic energy is not aparent.

Comparison with Mine Tremors from Different Source Regions

As outlined by Hanks and Thatcher (1972) and Thatcher (1972) the use of an $\Omega_0 - f_0$ diagram has the advantage that data comparison is independent of the scaling associated with a particular model. Ω_0 and f_0 are spectral parameters which do not depend on assumptions concerning wave velocity and density.

Horizontal lines in the $\Omega_0 - f_0$ plot are lines of constant Ω_0 and M_0. The vertical lines are lines of constant f_0 and r_0. Following Keilis-Borok (1957) and Brune (1970, 1971) the stress drop $\Delta\sigma_0$ can be written:

$$\Delta\sigma_0 = k\Omega_0 f_0^3 \tag{12}$$

where k is a contant factor. Lines with a slope -3 in the $\Omega_0 - f_0$ diagram are lines of constant $\Omega_0 \cdot f_0^3$ and $\Delta\sigma_0$. In the case of Brune's model the constant is given by $k = 106\rho R$. The actual value of $\Delta\sigma_0$ can be read from the diagram when Ω_0 and f_0 are known.

Figure 9 shows an $\Omega_0 - f_0$ plot with data from mine tremors of different source regions. The Ω_0-values are in all cases corrected for hypocentral distance and normalized to $R = 100$ km as indicated by $\Omega_{0(100)}$.

Spottiswoode and McGarr (1975) determined P- and S-wave spectra, In Fig. 9 only the parameters Ω_0 and f_0 of the P-wave spectra are used. Smith et al. (1974) and Gibbowicz and Chichowicz (1974) used S-wave spectra as did McGarr et al. (1981).

Hanks and Thatcher (1972) report the following relations between $\Omega_0(P)$ and $\Omega_0(S)$, determined from P- and S-wave spectra, respectively:
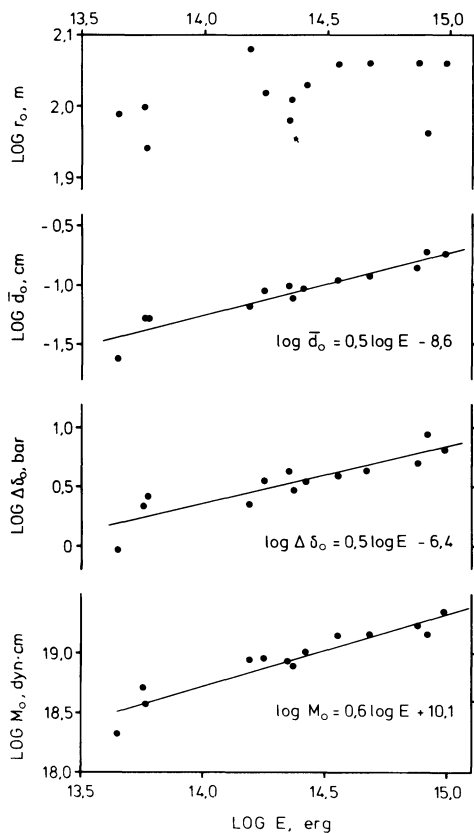
Fig. 8. From top to bottom: Source dimension r_0, average dislocation $\bar{d}_0$, stress drop $\Delta\sigma_0$, and seismic moment M_0 versus seismic energy E
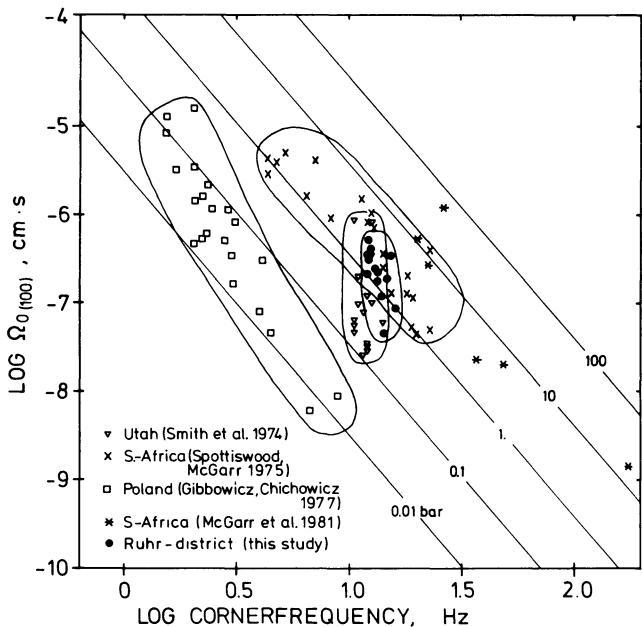

Fig. 9. $\Omega_0 - f_0$ diagram of source parameters from mine tremors. *Open triangles* ($\triangledown$) are data from Sunnyside coalmine, Utah (Smith et al., 1974); *crosses* represent data from a deep-level gold mine, South-Africa (Spottiswoode and McGarr 1975 ($\times$); McGarr et al. 1981 (+)); *open squares* ($\square$) are data from Polish coal mine (Gibbowicz and Chichowicz 1977); *circles* ($\bullet$) are data of this study from the eastern part of the Ruhr-district

$$\Omega_0(S) = (\alpha/\beta)^3 \, \Omega_0(P)$$
$$f_0(S) = \alpha/\beta f_0(P).$$

Gibbowicz and Chichowicz (1977) used a model of Madariaga (1976) to compute source dimensions. The dimensions derived from Madariaga's model are greater by about a factor of 2 than those calculated from Brune's model. Stress drops for Madariaga's model are one order of magnitude higher than those found with Brune's model due to the cube of the source dimension in the denominator of Eq. (11).

The data from different source regions form clusters in the $\Omega_0 - f_0$ plot.

The cluster of data points from Polish coal mines is nearly parallel to lines of contant stress drop between 0.01 and 0.1 bars. An increase in Ω_0 and M_0 is strongly connected with a decrease in the corner frequency as would be expected for an increase in source dimension. A significant increase of stress drop with an increase of Ω_0 is not seen.

A similar result can be derived from data of tremors in the deep level gold mine in South Africa. The stress drops are generally in the range of 1 to 10 bars. A stress drop of nearly 100 bars reported by McGarr et al. (1981) is an exception. Again an increase of Ω_0 and M_0 respectively is caused by an enlarged source dimension.

Data from the Sunnyside coal mine in Utah (Smith et al. 1974) show a very small variation of the corner frequency, and source dimension. An increase of Ω_0, M_0 is mainly caused by a larger stress drop. This has already been pointed out by Smith et al. (1974) in comparison with the relations between stress drop and seismic moment of these mine tremors and earthquake data from Wyss (1970) and Douglas and Ryall (1972).

Smith found higher stress drops and smaller source areas for the tremors in the Sunnyside district than for earthquakes of comparable seismic moment in Central Nevada. A possible reason for this is the higher regional stress in the Sunnyside district. The hypocenters of the tremors in the Sunnyside district are below the level of mine works (about 1 km) in contrast to other regions. Smith assumes that redistribution of stresses by unloading of coal induces submine earthquakes in response to the regional stress.

The tremors from the eastern part of the Ruhr-district cover only a small range of Ω_0, M_0. This may be one reason why no clear relation between seismic energy and source dimension was found (see Fig. 6). The cluster in Fig. 9 of type I events indicates a strong dependence of seismic moment on changes in stress drop, while there is only a very small variation in the corner frequency.

Summary

Far field spectra of mine tremors from the eastern part of the Ruhr-district appear to be very similar to earthquakes. The displacement spectra of P-pulses have generally a well defined low-frequency level and a decay of spectral amplitude beyond the corner frequency.

An average high-frequency asymptote proportional to f^{-3} is derived from the data. Following Savage (1972) this can indicate a far field displacement which

increases quadratically with time. In spite of the decay proportional for f^{-3} the Brune model, which yields a decay according to f^{-2}, has been chosen to derive physical parameters of the source for comparison with other studies.

Source dimensions of the tremors are in the range of 90–120 m, which is a realistic figure for the Ruhr-district. The length of the mine face decisively determines the dimension in which the local stress field is modified by mine works. The length of mine face which coincides with most of the epicenters (see Fig. 1), is actually 220 m.

The agreement of the data with the energy-magnitude relation given by Gutenberg und Richter (1956) also indicates some similarity between mine tremors and earthquakes.

The data of source dimension, stress drop, and seismic moment agree well with those found by Gibbowicz and Chichowicz, McGarr, Spottiswoode and McGarr, and Smith for other source regions. In some regions the seismic moment of an event is mainly determined by source size (for example in Polish coal mines and in the deep level mine in South Africa). In the Sunnyside district (Utah) and the eastern part of the Ruhr-district, stress drop is the dominating parameter.

References

Aki, K.. Generation and propagation of G-waves from the Niigata earthquake of June 16, 1964. Part 2. Estimation of earthquake moment, released energy, and stress-strain drop from the G-wave spectrum. Bull. Earthquake Res. Inst., Tokyo Univ. **44**, 73–78, 1966

Aki, K.: Scaling law of seismic spectrum. J. Geophys. Res. **72**, 1217–1231, 1967

Aki, K.: Source mechanism and earthquake prediction. Editions du Centre National de la Recherche Scientifique, 15, quai Anatole-France, Paris, pp. 23–50, 1980

Archambeau, C.B.: Elastodynamic source theory. Ph.D. thesis, Cal. Inst. Tech., Pasadena, 1964

Baule, H., Hinzen, K.-G.: Erfassung und Deutung von Erderschütterungen, insbesondere zur Ortung von Gebirgsschlägen. Schlußbericht i.A. des Landesoberbergamtes und Wirtschaftsministeriums NW. Inst. f. Geophys., Ruhr-Univ. Bochum, 1981

Berckhemer, H., Jacob, K.H.: Investigation of dynamical process in an earthquake foci by analyzing the pulse shape of body waves. Ber. Inst. Meteor. Geophys., Univ. Frankfurt/ Main, 13, 1968

Boatwright, J.: A spectral theory of circular seismic sources; simple estimates of source dimension, dynamic stress drop, and radiated seismic energy. Bull. Seism. Soc. Am. Vol. **70** (1), 1–26, 1980

Brune, J.N.. Tectonic stress and spectra of seismic shear waves from earthquakes. J. Geophys. Res. **75**, 4997–5009, 1970

Brune, J.N.. Tectonic stress and spectra of seismic shear waves from earthquakes. J. Geophys. Res. **76**, 5002, 1971

Casten, U., Cete, A.: Induzierte Seismizität im Bereich des Steinkohlenbergbaus des Ruhrreviers. Glückauf-Forschungshefte **41**, 12–16, 1980

Douglas, B.M., Ryall, A.: Spectral characteristics and stress drop for microearthquakes near Fairview Peak, Nevada. J. Geophys. Res. **77**, 351–359, 1972

Gibbowicz, S.J., Chichowicz, A.: Seismic moment and source size of mining tremors in Upper Silesia, Poland. Acta Geophysica, Polen **XXV**, 201–218, 1977

Gutenberg, B., Richter, C.F.: Magnitude and energy of earthquakes. Ann. Geofis. (Rome) **9**, 1–15, 1956

Hanks, T.C., Thatcher, W.: A graphical representation of seismic source parameters. J. Geophys. Res. **77**, 4393–4405, 1972

Hanks, T.C., Wyss, M.: The use of body-wave spectra in the determination of seismic-source parameters. Bull. Seism. Soc. Am. **62**, 561–589, 1972

Haskell, N.: Total energy and energy spectral density of elastic wave radiation from propagating faults. Bull. Seism. Soc. Am. **54**, 1811–1841, 1964

Kasahara, K.. The nature of seismic origins as inferred from seismological and geoelectric observations. Bull. Earthquake Res. Inst. Tokyo Univ. **35**, 473–530, 1957

Keilis-Borok, V.J.: Investigation of the mechanism of earthquakes (in Russian). Tr. Inst. Geofis. Akad. Nauk., SSSR, 40, 1957. (Engl. transl., Sov. Res. Geophys. Ser., 4, 1960)

Madariaga, R.: Dynamics of an expanding circular fault. Bull. Seism. Soc. Am. Vol. **66**, No. 3, 639–666, 1976

Madariaga, R.: Implications of stress-drop models of earthquakes for the inversion of stress drop from seismic observations. Pageoph. **115**, 301–316, 1977

Marion, G.E., Long, L.T.: Microearthquake spectra in the south eastern United States. Bull. Seism. Soc. Am. **70**, 1037–1054, 1980

McGarr, A., Green, R.W.E., Spottiswoode, S.M.: Strong motion of mine tremors: some implications for near-source ground motion parameters. Bull. Seism. Soc. Am. **71**, 295–320, 1981

McGarr, A., Spottiswoode, S.M., Gay, N.C. Ortlepp, W.D.: Observations relevant to seismic driving stress, stress drop, and efficiency. J. Geophys. Res. **84**, 2251–2261, 1979

Pelzing, R.: Untersuchungen zur Ortung von Herden seismischer Ereignisse, dargestellt an Beispielen aus einem Stationsnetz im Ruhrgebiet. Ber. Inst. für Geophys., Ruhr-Universität Bochum, Nr. 6, 1978

Perret, W.R.: Seismic source energies of underground nuclear explosions. Bull. Seism. Soc. Am. **62**, 763–774, 1972

Reid, H.F.: On mass movements in tectonic earthquakes and the depth of focus. Gerlands Beitr. Geophys. **10**, 318–351, 1910

Richter, C.F.: Elementary seismology. W.H. Freeman a.Co., San Francisco, 768 pp., 1958

Savage, J.C.: Relation of corner frequency to fault dimensions. J. Geophys. Res. **77**, 3788–3795, 1972

Smith, R.B., Winkler, P.L., Anderson, J.G., Scholz, C.H.. Source mechanisms of microearthquakes associated with underground mines in eastern Utah. Bull. Seism. Soc. Am. **64**, 1295–1317, 1974

Spottiswoode, S.M., McGarr, A.: Source parameters of tremors in a deep-level gold mine. Bull. Seism. Am. **65**, 93–112, 1975

Thatcher, W.: Regional variations of seismic source parameters in the northern Baja California area. J. Geophys. Res. **77**, 1549–1565, 1972

Thatcher, W., Hanks, T.: Source parameters of Southern California earthquakes. J. Geophys. Res. **78**, 8547–8576, 1973

Westbrook, G.K., Kasznir, N.J., Browitt, C.W.A., Holdsworth, B.K.: Seismicity induced by coal mining in Stoke-on-Trent (U.K.). Engin. Geol. **16**, 225–241, 1980

Wyss, M.. Stress estimates for South American shallow and deep earthquakes. J. Geophys. Res. **75**, 1529–1544, 1970